

## Self-assembly

SPECIAL  
ISSUE

# Simple and Versatile Preparation of Luminescent Amphiphilic Platinum(II)-containing Polystyrene Complexes With Transformable Nanostructures Assisted by Pt...Pt and $\pi$ - $\pi$ Interactions

Heung-Kiu Cheng, Clive Yik-Sham Chung, Kaka Zhang, and Vivian Wing-Wah Yam<sup>\*[a]</sup>

**Abstract:** Platinum(II)-containing polystyrene (PS) complexes have been synthesized by dehydrohalogenation of  $\alpha$ -alkyne-PS and chloroplatinum(II) precursors with different functionalities on the terpyridine ligands. Through modulation of the hydrophilicity/hydrophobicity of the terpyridine ligands and hence the overall amphiphilicity of the complexes, the complexes can undergo self-assembly into various superstructures with remarkable luminescence properties in different

solution mixtures, as revealed by electron microscopy, UV/Vis absorption and emission spectroscopy. Pt...Pt and/or  $\pi$ - $\pi$  interactions among the platinum(II) terpyridine moieties are found to play substantial roles in the stabilization of the superstructures and the turn-on/off of the triplet metal-metal-to-ligand charge transfer (<sup>3</sup>MMLCT) emission of the complexes.

## Introduction

Non-covalent supramolecular interactions have been demonstrated for the construction of highly ordered superstructures, which have had significant impact on the development of functional materials, catalysts and optoelectronics.<sup>[1-37]</sup> A particularly interesting class of molecules that can undergo supramolecular assembly is amphiphiles.<sup>[1-4,17-41]</sup> Amphiphiles consist of both hydrophilic and hydrophobic segments, and hence they can form superstructures driven by hydrophobic-hydrophobic interactions,  $\pi$ - $\pi$  interactions and/or hydrogen bonding in aqueous media.<sup>[1-3,18-36]</sup> In general, superstructures formed by amphiphilic polymers are more stable and robust than those formed by small molecules, owing to the superior physical and mechanical properties of polymeric materials.<sup>[25-34,38-41]</sup> Therefore, amphiphilic polymers have been exploited for numerous applications including the development of drug-delivery system, diagnostic imaging, nanoreactors and so on.<sup>[31-34]</sup> A common strategy for the preparation of amphi-

philic polymers is the use of controlled polymerization to form block copolymers. Different kinds of controlled polymerizations such as reversible addition-fragmentation chain transfer (RAFT) polymerization,<sup>[42]</sup> atom transfer radical polymerization (ATRP),<sup>[42,43]</sup> and ring-opening metathesis polymerization (ROMP),<sup>[44]</sup> have been developed in the recent decades to improve the ease of synthesis of block copolymers. Nevertheless, most of the multi-block copolymers still have a higher polydispersity compared to that of homopolymers.<sup>[45]</sup> As a result, the exploration of new classes of amphiphilic polymers through simple and versatile synthetic pathways can be advantageous for further development of self-assembled functional materials.

Pt...Pt interaction is an example of non-covalent interactions and can be found in sterically unhindered d<sup>8</sup> platinum(II) complexes.<sup>[1-16,46-60]</sup> With Pt...Pt and  $\pi$ - $\pi$  interactions, square-planar d<sup>8</sup> platinum(II) complexes can undergo self-assembly into a variety of superstructures, such as micelles,<sup>[2,3,8-10,16]</sup> vesicles,<sup>[1]</sup> nanorods,<sup>[1,2,4,5]</sup> nanorings,<sup>[5]</sup> helices,<sup>[4,13]</sup> fibers,<sup>[14,15]</sup> and metallo-gels.<sup>[6,7,11]</sup> More interestingly, the Pt...Pt and  $\pi$ - $\pi$  interactions can modulate the energy levels of d $\sigma^*$ (Pt<sub>n</sub>) and  $\pi^*$ (tridentate ligand) orbitals, and hence platinum(II) complexes with different extents of Pt...Pt and  $\pi$ - $\pi$  interactions show different spectroscopic and luminescence properties in their superstructures.<sup>[1-16]</sup> This has allowed the platinum(II) moieties to serve as spectroscopic and luminescence reporters of morphological transformations of superstructures.<sup>[1-16]</sup>

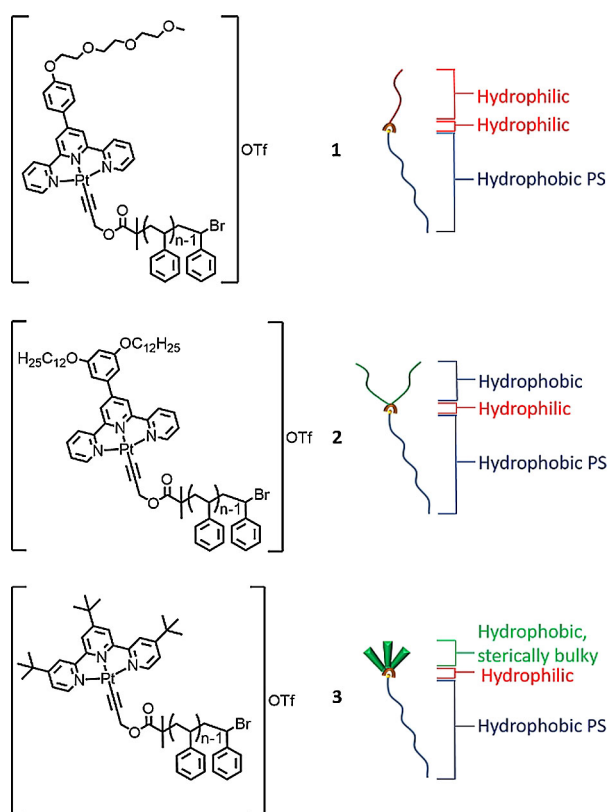
Recently, our group reported several classes of alkynylplatinum(II) terpyridine-based metallopolymers, and pH- and/or temperature-induced micellizations have been successfully probed by the changes in the UV/Vis and emission spectra of the complexes.<sup>[8-10]</sup> This suggests that terpyridine coordination

[a] H.-K. Cheng, Dr. C. Y.-S. Chung, Dr. K. Zhang, Prof. Dr. V. W.-W. Yam  
Institute of Molecular Functional Materials (Areas of Excellence Scheme,  
University Grants Committee (Hong Kong)) and Department of Chemistry  
The University of Hong Kong  
Pokfulam Road (Hong Kong)  
E-mail: wwyam@hku.hk

Supporting information and the ORCID identification number(s) for the author(s) of this article can be found under:  
<http://dx.doi.org/10.1002/asia.201700123>.

This manuscript is part of a special issue celebrating the 100th anniversary of the Royal Australian Chemical Institute (RACI). A link to the Table of Contents of the special issue will appear here when the complete issue is published.

onto a platinum(II) metal center and dehydrohalogenation of chloroplatinum(II) precursors with alkynes are promising synthetic strategies for the construction of metallopolymers. Nonetheless, the reported platinum(II)-based polymers have been shown to undergo self-assembly mainly based on the intrinsic properties of the polymeric materials, as no new superstructures can be found compared to those formed by the polymeric materials alone.<sup>[8–10,38–41]</sup> In view of the success in construction of interesting superstructures by Pt...Pt and  $\pi$ - $\pi$  interactions among platinum(II) polypyridine complexes,<sup>[1–16]</sup> it is conceivable that through judicious design, platinum(II)-based polymers can form dynamic superstructures assisted by Pt...Pt and  $\pi$ - $\pi$  interactions. Together with simple and versatile functionalization of terpyridine ligands, herein we report the synthesis and self-assembly study of amphiphilic block copolymer mimetics, which contain a hydrophobic polystyrene (PS) pendant, a hydrophilic positively charged platinum(II) center, and either hydrophilic (with triethylene glycol (TEG)) or hydrophobic (with long alkoxy chain or *tert*-butyl groups) terpyridine ligands (Scheme 1). The photophysical properties and morphological changes of the conjugates in different solvent systems have been investigated.



**Scheme 1.** Chemical structures and schematic drawing of hydrophilic and hydrophobic segments of **1**, **2** and **3**.

## Results and Discussion

### Synthesis and characterization

The structures of **1**, **2** and **3** and synthetic scheme are shown in Scheme 1 and Scheme S1 in the Supporting Information, respectively. Briefly,  $\alpha$ -alkyne-PS was prepared by ATRP, and was characterized by <sup>1</sup>H NMR and IR spectroscopies, and gel permeation chromatography (GPC). Subsequent copper(I)-catalyzed dehydrohalogenation of corresponding chloroplatinum(II) precursors with  $\alpha$ -alkyne-PS yielded the platinum(II)-containing PS complexes **1**, **2** and **3**. The complexes have been successfully characterized by <sup>1</sup>H NMR, IR and MALDI-TOF MS (Figures S1–S3). The MALDI-TOF MS data indicate a low polydispersity index (PDI; 1.03–1.05) of the complexes, similar to that of  $\alpha$ -alkyne-PS (1.07), demonstrating the promising preparation of versatile platinum(II)-containing PS complexes. Details of the synthesis and characterization data are included in the Experimental Section.

### Photophysical studies

The electronic absorption spectra of **1**, **2** and **3** in dioxane solution (0.1 mg mL<sup>-1</sup>) show an intense absorption at ca. 304–368 nm, and a lower-energy band at about 370–465 nm (Figure S4). According to previous studies,<sup>[1–16,46–60]</sup> the higher-energy intense absorption is assigned to the intraligand (IL)  $\pi \rightarrow \pi^*$  transitions of the terpyridine and alkynyl ligands, while the lower-energy absorption probably originates from a mixture of  $d\pi(\text{Pt}) \rightarrow \pi^*(\text{tpy})$  metal-to-ligand charge transfer (MLCT) and  $\pi(\text{alkynyl}) \rightarrow \pi^*(\text{tpy})$  ligand-to-ligand charge transfer (LLCT) transitions. In addition, concentration-dependent UV/Vis absorption spectra of all the complexes in dioxane follow Beer's law (Figures S5–S7), suggesting that there is no significant ground-state aggregation of the complexes in pure dioxane. Upon photoexcitation, **1** in dioxane (0.1 mg mL<sup>-1</sup>) shows yellow emission centered at 571 nm (Figure 1a), which is attributable to admixtures of <sup>3</sup>MLCT [ $d\pi(\text{Pt}) \rightarrow \pi^*(\text{tpy})$ ] and <sup>3</sup>LLCT [ $\pi(\text{alkynyl}) \rightarrow \pi^*(\text{tpy})$ ] states. Complexes **2** and **3** are found to be weakly emissive in dioxane solution (Figure 1b and 1c).

### Aggregation studies by addition of water

The effect of water addition to a solution of the complexes in dioxane was investigated. With increasing water content of the water–dioxane solution of **1** (0.1 mg mL<sup>-1</sup>), an emergence of a lower-energy absorption band at 460 nm is observed (Figure S8). In view of the decrease in absorbance at 460 nm at higher temperatures (Figure S9), this absorption band is tentatively assigned to metal–metal-to-ligand charge transfer (MMLCT) absorption, presumably through ground-state aggregation of **1** which brings the platinum(II) terpyridine units into close proximity, leading to Pt...Pt and/or  $\pi$ - $\pi$  interactions. Similar growth of temperature-dependent MMLCT absorption at 500 nm and hence ground-state aggregation is also observed in water–dioxane mixture of **2** with increasing water content (Figures S10 and S11). On the other hand, no significant UV/Vis

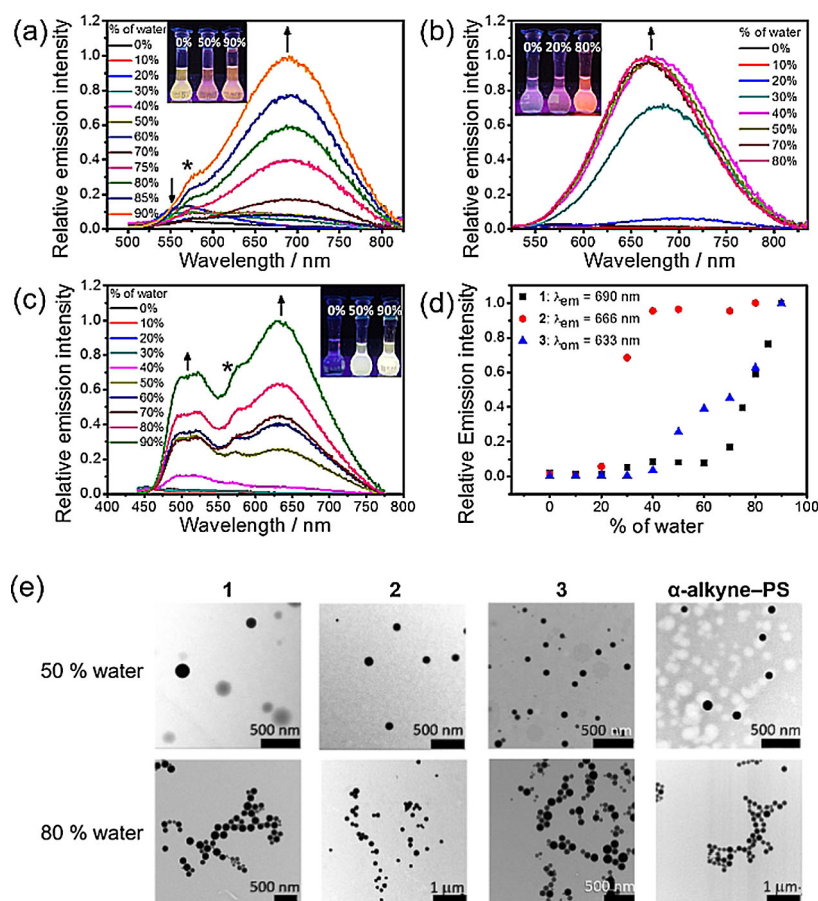


**Figure 1.** Emission spectra of (a) **1**, (b) **2** and (c) **3** in 1,4-dioxane ( $0.1 \text{ mg mL}^{-1}$ ) with increasing water content (the asterisk denotes an artifact). Insets: photographs of their emission colors. (d) Plot of emission intensity of the complexes against % of water in the water–dioxane mixture. (e) TEM images of **1**, **2**, **3** and  $\alpha$ -alkyne-PS in water–dioxane mixtures ( $0.1 \text{ mg mL}^{-1}$ ).

absorption spectral change is found in the water–dioxane solution of **3** ( $0.1 \text{ mg mL}^{-1}$ ) with increasing water content or temperature (Figures S12 and S13), indicating no ground-state aggregation of the complex. This can be rationalized by the presence of sterically bulky *tert*-butyl groups in **3**, hindering the self-assembly of the complex molecules.

The ground-state aggregation of **1**, **2** and **3** in water–dioxane mixtures has been further studied by transmission electron microscopy (TEM) and dynamic light scattering (DLS). No observable structures can be found in pure dioxane solution of the complexes, while all the complexes and  $\alpha$ -alkyne-PS form spherical micelles in 50% and 80% water–dioxane mixtures (Figure 1e), but with different sizes as revealed by DLS experiments (Table S1). Intensity-averaged hydrodynamic diameters ( $D_h$ ) of the micelles formed in 80% water–dioxane are in the order of **1** (176 nm) >  $\alpha$ -alkyne-PS (138 nm) > **2** (131 nm) > **3** (101 nm), and smaller  $D_h$  values were found in 80% water–dioxane mixtures as compared to those in 50% water–dioxane mixtures (Figure 2 and Table S1). The size decrease with increasing water composition was probably due to the reduction of dioxane content, which would lead to a more compact superstructure arising from the tendency to reduce the contact surface area with water. The similar structures of the spherical micelles of **1**, **2** and **3** as that of  $\alpha$ -alkyne-PS suggests that the

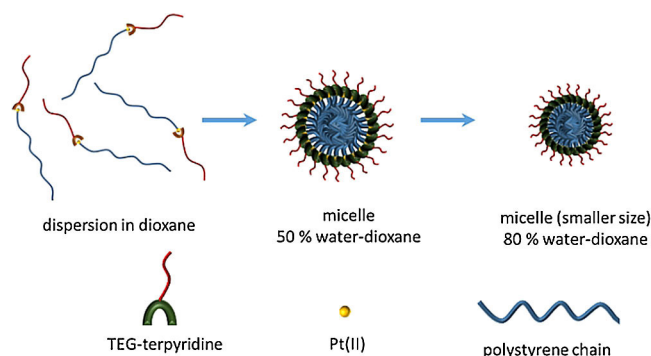


**Figure 2.** Schematic drawing of the formation of superstructures of **1** in different water–dioxane mixtures.

micellization is driven by the hydrophobic–hydrophobic interactions of the PS segment. In addition, the difference in the size of the micelles of different complexes indicates that micellization should be governed by other driving forces. Among the compounds studied, **1** was found to have the largest  $D_h$ . This can be explained by the higher solubility in a water–dioxane mixture due to the presence of the hydrophilic TEG pendant and a positively charged platinum(II) center, leading to the formation of less compact micelles compared to that of  $\alpha$ -

alkyne-PS. In contrast, **2** and **3** form smaller micelles than  $\alpha$ -alkyne-PS. Owing to the existence of hydrophobic long alkoxy chains and *tert*-butyl groups, stronger hydrophobic–hydrophobic interactions should be present in the micelles of **2** and **3**. This demonstrates that the amphiphilicity of the complexes plays a significant role in the self-assembly and hence the superstructures of the complexes, resembling the properties of reported block copolymers.<sup>[25–34]</sup> It is noteworthy that Pt...Pt and/or  $\pi$ – $\pi$  interactions among the terpyridine moieties of **1** and **2** are found in the 80% water–dioxane mixture, as revealed by UV/Vis absorption study (Figures S8–13), probably contributing to the micellization of **1** and **2**.

Interestingly, the superstructures of **1**, **2** and **3** show remarkable luminescence properties in water–dioxane mixtures upon photoexcitation. The yellow luminescence of **1** centered at 571 nm in water–dioxane mixtures of low water content is found to diminish and a concomitant growth of a red to near-infrared (NIR) emission band at 690 nm is observed with increasing water content (Figure 1a). With reference to previous related spectroscopic studies,<sup>[1–16,46–60]</sup> together with the observation of ground-state aggregation of **1** at high water content by TEM, UV/Vis absorption and DLS measurements, the monomeric complex molecules are believed to have undergone self-assembly into an aggregate species at high water content, leading to the drop of monomeric triplet <sup>3</sup>MLCT/LLCT emission at 571 nm with the emergence of the <sup>3</sup>MMLCT emission at 690 nm, typical of the aggregate species. The different emission origins have further been confirmed by excitation spectroscopic studies (Figure S14). Similarly, the red emission of **2** at 666 nm found at high water content is assigned to <sup>3</sup>MMLCT emission (Figure 1b), presumably through Pt...Pt and/or  $\pi$ – $\pi$  interactions among the aggregate molecules. Notably, **2** shows a turn-on of <sup>3</sup>MMLCT emission in the mixture with 30% or higher water content, while the growth of <sup>3</sup>MMLCT emission of **1** can only be found at 70% or higher water content (Figure 1d). This can be rationalized by the presence of hydrophobic alkoxy chains on the terpyridine ligand of **2**, resulting in stronger hydrophobic interactions and hence the formation of more compact spherical micelles, as revealed by TEM and DLS studies. This brings the complex molecules into closer proximity, leading to significant Pt...Pt and/or  $\pi$ – $\pi$  interactions, with <sup>3</sup>MMLCT emission observable at much lower water content when compared to **1** which has hydrophilic TEG pendants instead of the hydrophobic alkoxy chains. On the other hand, **3** is found to be dual-emissive at 522 and 633 nm (Figure 1c). Based on previous related photophysical studies,<sup>[1–16,46–60]</sup> the high-energy emission is ascribed to an admixture of <sup>3</sup>MLCT/LLCT emission origin. The close resemblance of the excitation spectra (Figure S15) monitored at the two emission bands together with the more prominent low-energy emission at higher water content suggest that the low-energy emission is of excimeric origin, although one cannot completely exclude the possible involvement of some <sup>3</sup>MMLCT character given the enhanced intensity of the excitation band in the wavelength range of 450–530 nm. The lack of MMLCT absorption in the UV/Vis absorption spectra of **3** in water–dioxane mixtures at high water content may suggest insignificant to rather weak

Pt...Pt and/or  $\pi$ – $\pi$  interactions, as revealed by the low to insignificant association constant in the ground state. Furthermore, the presence of the bulky *tert*-butyl groups may hinder the head-to-head stacking arrangement of the platinum(II) complexes, although a staggered arrangement of the *tert*-butyl groups between adjacent platinum(II) complexes is not unprecedented.<sup>[61,62]</sup> It is likely that both head-to-head and head-to-tail orientations would be possible upon aggregation at high water content, resulting in the co-existence of monomeric <sup>3</sup>MLCT/LLCT and excimeric emissions. The increase in intensities of both emission bands at higher water content might arise from the formation of compact micelles, which would rigidify the superstructured assemblies, reducing the rate of the non-radiative decay processes.

### Aggregation studies by addition of hexane

To further investigate the effect of hydrophilic and hydrophobic segments on the platinum(II)-PS complexes, the photo-physical and self-assembly properties of the complexes in non-polar solvent mixtures are studied. Upon addition of hexane into the dioxane solution of **1**, the UV/Vis absorption spectra revealed a decrease of the MLCT/LLCT absorption band at 428 nm and an increase of the MMLCT absorption shoulder at ca. 460 nm, with a well-defined isosbestic point at 453 nm (Figure S16). Together with the temperature dependence of the MMLCT absorption of **1** in a 70% hexane–dioxane mixture (Figure S17), **1** is believed to have undergone ground-state aggregation in the hexane–dioxane mixture, leading to Pt...Pt and/or  $\pi$ – $\pi$  interactions among the complex molecules. The decrease in the <sup>3</sup>MLCT/LLCT emission intensity at 571 nm and the emergence of <sup>3</sup>MMLCT emission at 705 nm with increasing hexane content further support the notion of ground-state aggregation of **1** at high hexane content (Figure 3a). Similar UV/Vis absorption and emission spectral changes are also observed in the study of **2** with increasing hexane content (Figure 3b and S18), suggesting the presence of Pt...Pt and/or  $\pi$ – $\pi$  interactions in the aggregates of **2**. The turn-on of <sup>3</sup>MMLCT emission of **1** is found at lower hexane content than that of **2** (Figure 3a and 3b), which is different from that observed in water–dioxane mixtures (Figure 1a and 1d). This can be explained by the lower solubility of **1** in hexane imparted by the hydrophilic TEG pendant, as compared to that of **2** which possesses the hydrophobic alkoxy chains, thus favoring the aggregation of **1** in hexane–dioxane mixtures. This demonstrates the importance of the balance of hydrophilicity/hydrophobicity of the complexes in dictating the photophysical and self-assembly properties of the complexes. For **3**, as only minimal changes in the UV/Vis absorption and emission spectra with increasing hexane content are observed (Figures S19–S21), no significant Pt...Pt and/or  $\pi$ – $\pi$  interactions should be found among the complex molecules in the hexane–dioxane mixtures, probably due to the steric hindrance from the *tert*-butyl groups on the terpyridine ligand.

Interestingly, TEM images reveal different superstructures formed by **1**, **2** and **3** in hexane–dioxane solution mixtures (Figure 3c). While  $\alpha$ -alkyne-PS shows no well-defined super-

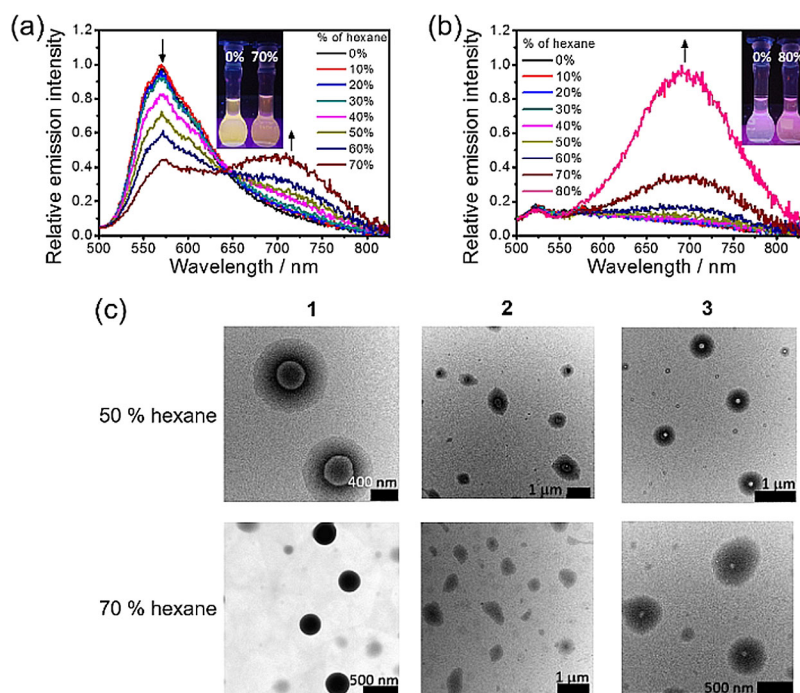


**Figure 3.** Emission spectra of (a) **1** and (b) **2** in 1,4-dioxane ( $0.1 \text{ mg mL}^{-1}$ ) with increasing hexane content. Insets: photographs of their emission colors. (c) TEM images of **1**, **2** and **3** in hexane–dioxane mixtures ( $0.1 \text{ mg mL}^{-1}$ ).

structures in these solution mixtures, **1** is found to form spherical multilayer structures ( $D_h = 670 \text{ nm}$  from DLS; Table S2) at 50% hexane content, and these multilayer structures transform into compact spherical micelles at 70% hexane content (Figure 3c). On the other hand, TEM images of **3** in both 50 and 70% hexane–dioxane solutions show hollow spherical structures with similar sizes (Table S2), and irregular aggregates of **2** are observed in hexane–dioxane solutions (Figure 3c).

Based on the results of UV/Vis absorption, emission, TEM and DLS studies, the proposed mechanisms for the self-assembly of **1**, **2** and **3** in hexane–dioxane solution mixtures are depicted in Figure 4. In view of the poor solvation of the hydrophilic TEG of **1** in hexane, **1** would form spherical structures in the 50% hexane–dioxane mixture with the hydrophobic PS forming the shell and the hydrophilic TEG pendant constituting the core. The sharp contrast of the ring-like structure in between the core and the shell should be attributed to the presence of the platinum(II) metal center, supporting the alignment of the complex molecules into the proposed structures as shown in Figure 4a. The presence of platinum(II) was further supported by energy-dispersive X-ray (EDX) analysis (Figure S22). It is worth noting that Pt–Pt and/or  $\pi$ – $\pi$  interactions are found in the solution of **1** at 50% hexane content, as revealed by the UV/Vis absorption and emission spectra. Therefore, Pt–Pt and/or  $\pi$ – $\pi$  interactions should contribute to the formation of these spherical multilayer structures. On the other hand, the multilayer structures of **1** at 50% hexane are found to shrink to form compact spherical micelles, leading to the turn-on of  $^3\text{MMLCT}$  emission centered at 705 nm when the hexane content is increased to 70%. This can be corroborated with the well-known poor solubility of PS in solutions with

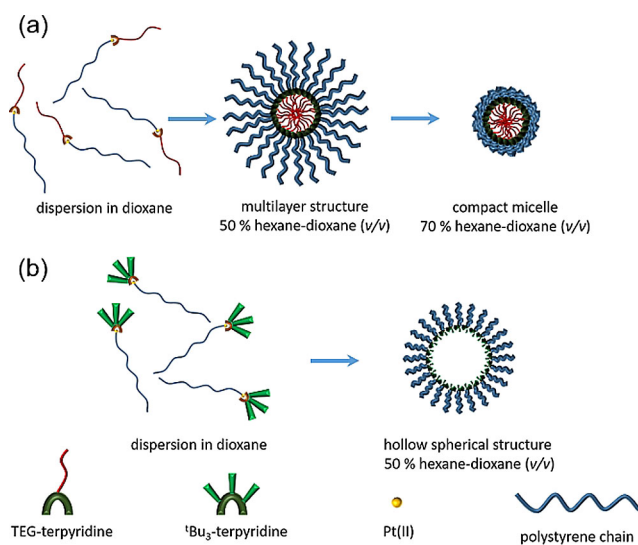


**Figure 4.** Schematic drawing of the formation of superstructures of (a) **1** and (b) **3** in different hexane–dioxane mixtures.

high hexane content,<sup>[63]</sup> together with the strong Pt–Pt and/or  $\pi$ – $\pi$  interactions among the complex molecules (Figures 3 and 4). The shrinkage of the superstructures at 70% hexane content, as compared to those observed at 50% hexane, is further supported by DLS experiments (Table S2). For **2**, only irregular aggregates are observed in the TEM images at both 50 and 70% hexane content (Figure 3c). This can be explained by the better solvating power in hexane–dioxane solution provided by the two large hydrophobic segments (PS and alkoxy chains), and the absence of strong hydrophobic–hydrophobic

interactions as driving force to form other well-defined aggregates. On the other hand, hollow spherical structures can be found in the 50% hexane–dioxane solution of **3** (Figure 4b). This formation can be contributed by the sterically bulky *tert*-butyl groups on **3** which hinder close packing of the platinum(II) terpyridine moieties. Further increase in hexane content of the solution of **3** only results in the formation of similar hollow spherical structures, and no morphological transformation, as in the study of **1**, can be found. This may arise from the absence of Pt...Pt,  $\pi$ - $\pi$  and hydrophobic–hydrophobic interactions among the complex **3** molecules, and hence compact superstructures cannot be formed. Together with the UV/Vis absorption and emission studies of **3** (Figures S19–S21), it is believed that the bulky *tert*-butyl groups would hinder the close packing of the platinum(II) units, which in the absence of other non-covalent interactions, results in no MMLCT emission or excimer emission upon increasing the hexane content. Therefore, **3** would remain weakly emissive at high hexane content (Figure S21).

## Conclusions

In conclusion, through simple and versatile functionalization of the terpyridine ligand and promising alkyne coordination, a new class of luminescent amphiphilic alkynylplatinum(II) terpyridine–polystyrene complexes has been designed and synthesized. With systematic tuning of the balance of hydrophilicity and hydrophobicity, the complexes are shown to undergo self-assembly into different superstructures by the systematic variation of the solvent composition, similar to that of amphiphilic block copolymers. In addition to hydrophobic–hydrophobic interactions which are the main driving forces for the self-assembly of amphiphilic block copolymers, the Pt...Pt and/or  $\pi$ - $\pi$  interactions among the platinum(II) terpyridine moieties have allowed the complexes to form transformable superstructures with unique luminescence turn-on and spectroscopic changes. The present work should provide insights into the design of new classes of luminescent amphiphilic materials which can be applicable in the area of nanotechnology and biomedical diagnostics. Moreover, it should open up a new strategy to prepare block copolymer mimetics by the introduction of promising metal-ligand coordination for the development of new functional materials.

## Experimental Section

**Materials and Reagents.** Propargyl alcohol, 2-bromo-2-methylpropionyl bromide, styrene, *N,N,N',N',N'*-pentamethyldiethylenetriamine (PMDETA), 1,4-dioxane (spectrophotometric grade,  $\geq 99\%$ ) were purchased from Sigma–Aldrich Co. Ltd. Triethylamine was purchased from Acros Organic Company. Copper(I) bromide (CuBr) was purchased from AK Scientific. 2-Acetylpyridine was purchased from Alfa Aesar. Styrene was purified by passing through basic aluminum oxide to remove any stabilizers before use. Triethylamine was distilled under  $N_2$  atmosphere before use. Propargyl 2-bromoisobutyrate,<sup>[64]</sup> tri(ethylene glycol) monomethyl ether tosylate,<sup>[65]</sup> 4-[tri(ethylene glycol) monomethyl ether]benzaldehyde<sup>[66]</sup> were synthesized according to reported procedures. All other reagents were

of analytical grade and were used without further purification. The reactions were performed under  $N_2$  atmosphere using standard Schlenk techniques unless specified otherwise.

**Physical Measurements and Instrumentation.**  $^1H$  NMR spectra were recorded with a Bruker AVANCE 400 (400 MHz) or DPX-300 (300 MHz) Fourier transform NMR spectrometer at room temperature with tetramethylsilane ( $Me_4Si$ ) as the internal reference. Positive-ion FAB mass spectra were recorded on a Thermo Scientific DFS high-resolution magnetic sector mass spectrometer. MALDI-TOF-MS were recorded by using an Autoflex Bruker MALDI-TOF MS system using *trans*-2-[3-(4-*tert*-butylphenyl)-2-methyl-2-propenyldene]malononitrile (DCTB) as the matrix. IR spectra were obtained as KBr disks by using a Bio-Rad FTS-7 FTIR spectrometer ( $4000$ – $400\text{ cm}^{-1}$ ). Elemental analyses of the platinum(II) complexes were performed on a Flash EA 1112 elemental analyzer at the Institute of Chemistry, Chinese Academy of Sciences. Measurements of molecular mass and molecular mass distribution of  $\alpha$ -alkyne-PS were performed at  $30^\circ C$  on Waters 1500 Series gel permeation chromatography (GPC) system equipped with two Waters 515 HPLC pumps, a Waters 2414 refractive index detector, a 2998 photodiode array detector and a Styragel HR 3 THF column. Polystyrenes with narrow molecular weight distribution were used as calibration standards. THF was used as an eluent at a flow rate of  $1.0\text{ mL min}^{-1}$ . Steady-state excitation and emission spectra were recorded on a SPEX Fluorolog-3 model FL3-211 fluorescence spectrofluorometer equipped with an R2658P PMT detector. The UV-visible spectra were obtained by using a Cary 50 (Varian) spectrophotometer equipped with a Xenon flash lamp. Dynamic light scattering (DLS) measurements were performed at ambient temperature using a Zetasizer 3000HSA with internal HeNe laser ( $\lambda_0 = 632.8\text{ nm}$ ) from Malvern (UK). Transmission electron microscopy (TEM) and the energy-dispersive X-ray (EDX) experiments were performed on a Philips CM100 transmission electron microscope with an accelerating voltage of 200 kV or a Philips Tecnai G2 20 S-TWIN transmission electron microscope with an accelerating voltage of 200 kV at the Electron Microscope Unit of The University of Hong Kong. The TEM samples were prepared by drop-casting dilute solutions onto a carbon-coated copper grid which was then allowed to undergo slow evaporation of the solvents in air for about 15 minutes.

## Synthesis

**$\alpha$ -Alkyne-PS.** The polymer was synthesized according to a reported method.<sup>[67]</sup> Yield: 5.5 g (52%).  $^1H$  NMR (400 MHz,  $CDCl_3$ , 298 K, relative to  $Me_4Si$ ):  $\delta = 0.95$ – $0.97$  (br,  $-C(CH_3)_2-$ ),  $1.43$ – $2.00$  (br, backbone  $-CH_2-$  and  $-CH-$ ),  $4.00$ – $4.40$  (br,  $-C\equiv C-CH_2-$ ,  $-C\equiv C-H$ ),  $6.20$ – $7.20$  ppm (br, phenyl). IR (KBr disk):  $\tilde{\nu} = 2130\text{ cm}^{-1}$  ( $w$ ;  $\nu(C\equiv C)$ ). GPC (versus polystyrene in THF):  $M_n = 2686\text{ Da}$ ,  $M_w = 2873\text{ Da}$ , PDI = 1.07.

**4'-[Tri(ethylene glycol) monomethyl ether]phenyl]-2,2':6',2''-terpyridine (tpy- $C_6H_4$ -TEG).** It was synthesized according to a literature procedure for a related terpyridine.<sup>[68]</sup> Yield: 3.6 g (35%).  $^1H$  NMR (400 MHz,  $CDCl_3$ , 298 K, relative to  $Me_4Si$ ):  $\delta = 3.38$  (s, 3H,  $-CH_3$ ),  $3.50$ – $3.76$  (m, 8H,  $-OCH_2-$ ),  $3.91$  (t,  $J = 4.7\text{ Hz}$ , 2H,  $-OCH_2-$ ),  $4.20$  (t,  $J = 4.7\text{ Hz}$ , 2H,  $-OCH_2-$ ),  $7.05$  (d,  $J = 8.8\text{ Hz}$ , 2H,  $-C_6H_4-$ ),  $7.34$  (m, 2H,  $-C_6H_4-$ ),  $7.84$ – $7.90$  (m, 4H, tpy),  $8.65$ – $8.74$  ppm (m, 6H, tpy). Positive FAB-MS:  $m/z = 472.0\text{ [M+H]}^+$ .

**4'-[3,5-Bis(dodecyloxy)phenyl]-2,2':6',2''-terpyridine (tpy- $C_6H_3$ - $(OC_{12}H_{25})_2$ -3,5).** It was synthesized according to a literature procedure for a related terpyridine.<sup>[4]</sup> Yield: 3.1 g (56%).  $^1H$  NMR (400 MHz,  $CDCl_3$ , 298 K, relative to  $Me_4Si$ ):  $\delta = 0.88$  (t,  $J = 6.3\text{ Hz}$ , 6H,  $-CH_3$ ),  $1.20$ – $1.40$  (m, 40H,  $-CH_2-$ ),  $4.04$  (t,  $J = 6.3\text{ Hz}$ , 4H,  $-OCH_2-$ ),  $6.55$  (s, 1H,  $-C_6H_3-$ ),  $7.00$  (s, 2H,  $-C_6H_3-$ ),  $7.35$  (t,  $J = 8.0\text{ Hz}$ , 2H,

tpy), 7.88 (t,  $J=8.0$  Hz, 2H, tpy), 8.65–9.73 ppm (m, 6H, tpy). Positive FAB-MS:  $m/z=678.6$   $[M+H]^+$ .

**[Pt(tpy-C<sub>6</sub>H<sub>4</sub>-TEG)Cl]OTf.** It was synthesized according to modification of a literature procedure for [Pt(tpy)Cl]OTf,<sup>[50,53]</sup> using tpy-C<sub>6</sub>H<sub>4</sub>-TEG (246 mg) instead of tpy. The final product was obtained as an orange solid. Yield: 300 mg (87%). <sup>1</sup>H NMR (400 MHz, CDCl<sub>3</sub>, 298 K, relative to Me<sub>4</sub>Si):  $\delta=3.37$  (s, 3H, -CH<sub>3</sub>), 3.50–3.76 (m, 8H, -OCH<sub>2</sub>-), 3.86 (t,  $J=4.8$  Hz, 2H, -OCH<sub>2</sub>-), 4.11 (t,  $J=4.8$  Hz, 2H, -OCH<sub>2</sub>-), 6.63 (d,  $J=8.0$  Hz, 2H, -C<sub>6</sub>H<sub>4</sub>-), 7.73 (t,  $J=8.0$  Hz, 2H, tpy), 7.89 (d,  $J=8.0$  Hz, 2H, -C<sub>6</sub>H<sub>4</sub>-), 8.30 (d,  $J=8.0$  Hz, 2H, tpy), 8.41 (s, 2H, tpy), 8.73 (d,  $J=8.0$  Hz, 2H, tpy), 9.05 ppm (d,  $J=5.0$  Hz, 2H, tpy). Positive FAB-MS:  $m/z=702.1$   $[M-OTf]^+$ . Elemental analysis calcd (%) for C<sub>29</sub>H<sub>29</sub>ClF<sub>3</sub>N<sub>3</sub>O<sub>7</sub>PtS·H<sub>2</sub>O: C, 40.07; H, 3.59; N, 4.83. Found: C, 40.16; H, 3.19; N, 5.02.

**[Pt(tpy-C<sub>6</sub>H<sub>3</sub>-(OC<sub>12</sub>H<sub>25</sub>)<sub>2</sub>-3,5)Cl]OTf.** It was synthesized according to modification of a literature procedure for [Pt(tpy)Cl]OTf,<sup>[50,53]</sup> using tpy-C<sub>6</sub>H<sub>3</sub>-(OC<sub>12</sub>H<sub>25</sub>)<sub>2</sub>-3,5 (171 mg) instead of tpy. The final product was obtained as a yellow solid. Yield: 294 mg (92%). <sup>1</sup>H NMR (400 MHz, CDCl<sub>3</sub>, 298 K, relative to Me<sub>4</sub>Si):  $\delta=0.88$  (t,  $J=6.4$  Hz, 6H, -CH<sub>3</sub>), 1.20–1.40 (m, 40H, -CH<sub>2</sub>-), 3.86 (t,  $J=6.4$  Hz, 4H, -OCH<sub>2</sub>-), 6.24 (s, 1H, -C<sub>6</sub>H<sub>3</sub>-), 6.82 (s, 2H, -C<sub>6</sub>H<sub>3</sub>-), 7.72 (t,  $J=8.0$  Hz, 2H, tpy), 8.40 (t,  $J=8.0$  Hz, 2H, tpy), 8.44 (s, 2H, tpy), 8.89 (d,  $J=8.0$  Hz, 2H, tpy), 9.12 ppm (d,  $J=4.7$  Hz, 2H, tpy). Positive FAB-MS:  $m/z=908.6$   $[M-OTf]^+$ . Elemental analysis calcd (%) for C<sub>46</sub>H<sub>63</sub>ClF<sub>3</sub>N<sub>3</sub>O<sub>5</sub>PtS·H<sub>2</sub>O·CH<sub>2</sub>Cl<sub>2</sub>: C, 48.64; H, 5.82; N, 3.62. Found: C, 48.73; H, 5.69; N, 3.56.

**[Pt(tpy-C<sub>6</sub>H<sub>4</sub>-TEG){C≡CCH<sub>2</sub>OC(=O)C(CH<sub>3</sub>)<sub>2</sub>PS}]OTf (1).** It was synthesized by dehydrohalogenation reaction of [Pt(tpy-C<sub>6</sub>H<sub>4</sub>-TEG)Cl]OTf (142 mg) and  $\alpha$ -alkyne-PS (500 mg) in the presence of CuI as the catalyst in dichloromethane (10 mL) and distilled triethylamine (1 mL) using a modification of a literature procedure for [Pt(tpy){C≡CC<sub>6</sub>H<sub>5</sub>}OTf.<sup>[7,69]</sup> The crude product was dissolved in dichloromethane and any undissolved solid was filtered off. The filtrate was purified by using column chromatography on silica gel. The product was obtained as a red solid, and then washed with hot methanol and hexane for a few times, and dried in vacuum. Yield: 320 mg (51%). <sup>1</sup>H NMR (300 MHz, CDCl<sub>3</sub>, 298 K, relative to Me<sub>4</sub>Si):  $\delta=0.75$ –1.15 (br, -C(CH<sub>3</sub>)<sub>2</sub>-), 1.15–2.15 (br, backbone -CH<sub>2</sub>- and -CH-), 3.37 (br, 3H, -OCH<sub>3</sub>), 3.50–3.60 (br, 2H, -OCH<sub>2</sub>-), 3.60–3.80 (br, 8H, -OCH<sub>2</sub>-), 3.80–4.00 (br, 2H, -OCH<sub>2</sub>-), 4.00–4.50 (br, -C≡C-CH<sub>2</sub>-), 6.25–7.25 (br, phenyl protons of polystyrene and -C<sub>6</sub>H<sub>4</sub>-), 7.48 (br, 2H, tpy), 8.00 (br, 4H, tpy and -C<sub>6</sub>H<sub>4</sub>-), 8.22 (br, 2H, tpy), 8.60 (br, 2H, tpy), 8.99 ppm (br, 2H, tpy). IR (KBr disk):  $\tilde{\nu}=2145$  cm<sup>-1</sup> (w;  $\nu$ (C≡C)). MALDI-TOF MS:  $M_n=3775$  Da,  $M_w=3878$  Da, PDI=1.03.

**[Pt(tpy-C<sub>6</sub>H<sub>3</sub>-(OC<sub>12</sub>H<sub>25</sub>)<sub>2</sub>-3,5){C≡CCH<sub>2</sub>OC(=O)C(CH<sub>3</sub>)<sub>2</sub>PS}]OTf (2).** The procedure was similar to that used to prepare 1, except that [Pt(tpy-C<sub>6</sub>H<sub>3</sub>-(OC<sub>12</sub>H<sub>25</sub>)<sub>2</sub>-3,5)Cl]OTf (101 mg) was used instead of [Pt(tpy-C<sub>6</sub>H<sub>4</sub>-TEG)Cl]OTf. The product was obtained as a yellow solid. Yield: 210 mg (57%). <sup>1</sup>H NMR (300 MHz, CDCl<sub>3</sub>, 298 K, relative to Me<sub>4</sub>Si):  $\delta=0.75$ –1.15 (br, -C(CH<sub>3</sub>)<sub>2</sub>- and -CH<sub>3</sub>), 1.20–2.20 (br, backbone -CH<sub>2</sub>- and -CH-), 3.93 (br, 4H, -OCH<sub>2</sub>-), 4.20–4.60 (br, -C≡C-CH<sub>2</sub>-), 6.24 (br, 1H, -C<sub>6</sub>H<sub>3</sub>-), 6.25–7.10 (br, phenyl protons of polystyrene and -C<sub>6</sub>H<sub>3</sub>-), 7.49 (br, 2H, tpy), 8.31 (br, 2H, tpy), 8.51 (br, 2H, tpy), 8.92 (br, 2H, tpy), 9.07 ppm (br, 2H, tpy). IR (KBr disk):  $\tilde{\nu}=2145$  cm<sup>-1</sup> (w;  $\nu$ (C≡C)). MALDI-TOF MS:  $M_n=3381$  Da,  $M_w=3353$  Da, PDI=1.05.

**[Pt(tBu<sub>3</sub>tpy){C≡CCH<sub>2</sub>OC(=O)C(CH<sub>3</sub>)<sub>2</sub>PS}]OTf (3).** The procedure was similar to that used to prepare 1, except that [Pt(tBu<sub>3</sub>tpy)Cl]OTf (122 mg) was used instead of [Pt(tpy-C<sub>6</sub>H<sub>4</sub>-TEG)Cl]OTf. The product was obtained as a yellow solid. Yield: 400 mg (69%). <sup>1</sup>H NMR (400 MHz, CDCl<sub>3</sub>, 298 K, relative to Me<sub>4</sub>Si):  $\delta=0.90$ –1.10 (br, -C(CH<sub>3</sub>)<sub>2</sub>-), 1.20–2.00 (br, backbone -CH<sub>2</sub>- and -CH-),

2.16 (s, 27H, -tBu), 4.20–4.60 (br, -C≡C-CH<sub>2</sub>-), 6.25–7.25 (br, phenyl protons of polystyrene), 7.47 (br, 2H, tpy), 8.39 (br, 2H, tpy), 8.46 (br, 2H, tpy), 8.97 ppm (br, 2H, tpy). IR (KBr disk):  $\tilde{\nu}=2143$  cm<sup>-1</sup> (w;  $\nu$ (C≡C)). MALDI-TOF MS:  $M_n=3703$  Da,  $M_w=3829$  Da, PDI=1.03.

## Acknowledgements

V.W.-W.Y. acknowledges the support from the University Grants Committee Areas of Excellence (AoE) Scheme (AoE/P-03/08) and a General Research Fund (GRF) grant from the Research Grants Council of Hong Kong Special Administrative Region, P. R. China (HKU17304715). H.-K.C. acknowledges the receipt of a Postgraduate Studentship. We are thankful to Prof. R.W.-Y. Wong and Dr. C.-L. Ho for access to the MALDI-TOF-MS characterization facilities at the Hong Kong Baptist University. We also thank Mr. F.Y.-F. Chan at the Electron Microscope Unit of The University of Hong Kong for helpful technical assistance.

**Keywords:** metal–metal interactions • platinum • polymers • self-assembly • supramolecular chemistry

- [1] C. Po, A. Y.-Y. Tam, K. M.-C. Wong, V. W.-W. Yam, *J. Am. Chem. Soc.* **2011**, *133*, 12136–12143.
- [2] C. Po, A. Y.-Y. Tam, V. W.-W. Yam, *Chem. Sci.* **2014**, *5*, 2688–2695.
- [3] C. Po, V. W.-W. Yam, *Chem. Sci.* **2014**, *5*, 4868–4872.
- [4] S. Y.-L. Leung, K. M.-C. Wong, V. W.-W. Yam, *Proc. Natl. Acad. Sci. USA* **2016**, *113*, 2845–2850.
- [5] H.-L. Au-Yeung, S. Y.-L. Leung, A. Y.-Y. Tam, V. W.-W. Yam, *J. Am. Chem. Soc.* **2014**, *136*, 17910–17913.
- [6] A. Y.-Y. Tam, K. M.-C. Wong, V. W.-W. Yam, *J. Am. Chem. Soc.* **2009**, *131*, 6253–6260.
- [7] A. Y.-Y. Tam, K. M.-C. Wong, G. Wang, V. W.-W. Yam, *Chem. Commun.* **2007**, 2028–2030.
- [8] C. Y.-S. Chung, V. W.-W. Yam, *Chem. Eur. J.* **2013**, *19*, 13182–13192.
- [9] Y. Hu, K. H.-Y. Chan, C. Y.-S. Chung, V. W.-W. Yam, *Dalton Trans.* **2011**, *40*, 12228–12234.
- [10] V. W.-W. Yam, Y. Hu, K. H.-Y. Chan, C. Y.-S. Chung, *Chem. Commun.* **2009**, 6216–6218.
- [11] X.-S. Xiao, W. Lu, C.-M. Che, *Chem. Sci.* **2014**, *5*, 2482–2488.
- [12] Y. Chen, C.-M. Che, W. Lu, *Chem. Commun.* **2015**, *51*, 5371–5374.
- [13] A. Aliprandi, C. M. Croisetu, M. Mauro, L. D. Cola, *Chem. Eur. J.* **2017**, *23*, DOI: 10.1002/chem.201605103.
- [14] M. Mauro, A. Aliprandi, C. Cebrino, D. Wang, C. Kubel, L. De Cola, *Chem. Commun.* **2014**, *50*, 7269–7272.
- [15] M. E. Robinson, D. J. Lunn, A. Nazemi, G. R. Whittell, L. De Cola, I. Manners, *Chem. Commun.* **2015**, *51*, 15921–15924.
- [16] F.-W. Liu, L.-Y. Niu, Y. Chen, V. Ramamurthy, L.-Z. Wu, C.-H. Tung, Y.-Z. Chen, Q.-Z. Yang, *Chem. Eur. J.* **2016**, *22*, 18132–18139.
- [17] F. J. M. Hoeben, P. Jonkheijm, E. W. Meijer, A. P. H. J. Schenning, *Chem. Rev.* **2005**, *105*, 1491–1546.
- [18] J.-M. Lehn, *Science* **2002**, *295*, 2400–2403.
- [19] T. Aida, E. W. Meijer, S. I. Stupp, *Science* **2012**, *335*, 813–817.
- [20] J. D. Hartgerink, E. Beniash, S. I. Stupp, *Science* **2001**, *294*, 1684–1688.
- [21] J.-M. Lehn, *Proc. Natl. Acad. Sci. USA* **2002**, *99*, 4763–4768.
- [22] J.-M. Lehn, *Chem. Soc. Rev.* **2007**, *36*, 151–160.
- [23] R. Chakrabarty, P. S. Mukherjee, P. J. Stang, *Chem. Rev.* **2011**, *111*, 6810–6918.
- [24] B. H. Northrop, Y.-R. Zheng, K.-W. Chi, P. J. Stang, *Acc. Chem. Res.* **2009**, *42*, 1554–1563.
- [25] L. Zhang, A. Eisenberg, *Science* **1995**, *268*, 1728–1731.
- [26] Y. Yu, L. Zhang, A. Eisenberg, *Macromolecules* **1998**, *31*, 1144–1154.
- [27] L. Zhang, A. Eisenberg, *Macromolecules* **1996**, *29*, 8805–8815.
- [28] X. F. Zhong, S. K. Varshney, A. Eisenberg, *Macromolecules* **1992**, *25*, 7160–7167.

- [29] K. Yu, L. Zhang, A. Eisenberg, *Langmuir* **1996**, *12*, 5980–5984.
- [30] L. Zhang, A. Eisenberg, *J. Am. Chem. Soc.* **1996**, *118*, 3168–3181.
- [31] D. E. Discher, A. Eisenberg, *Science* **2002**, *297*, 967–973.
- [32] M. Moffitt, K. Khougaz, A. Eisenberg, *Acc. Chem. Res.* **1996**, *29*, 95–102.
- [33] Y. Mai, L. Xiao, A. Eisenberg, *Macromolecules* **2013**, *46*, 3183–3189.
- [34] Y. Mai, A. Eisenberg, *Chem. Soc. Rev.* **2012**, *41*, 5969–5985.
- [35] M. Ramanathan, L. K. Shrestha, T. Mori, Q. Ji, J. P. Hill, K. Ariga, *Phys. Chem. Chem. Phys.* **2013**, *15*, 10580–10611.
- [36] C. Fong, T. Le, C. J. Drummond, *Chem. Soc. Rev.* **2012**, *41*, 1297–1322.
- [37] A. S. Tayi, A. Kaeser, M. Matsumoto, T. Aida, S. I. Stupp, *Nat. Chem.* **2015**, *7*, 281–294.
- [38] C. Guo, J. Wang, H.-Z. Liu, J.-Y. Chen, *Langmuir* **1999**, *15*, 2703–2708.
- [39] Q. Guo, R. Thomann, W. Gronski, T. Thurn-Albrecht, *Macromolecules* **2002**, *35*, 3133–3144.
- [40] C. Sommer, J. S. Pedersen, P. C. Stein, *J. Phys. Chem. B* **2004**, *108*, 6242–6249.
- [41] J.-H. Ma, C. Guo, Y.-L. Tang, H.-Z. Liu, *Langmuir* **2007**, *23*, 9596–9605.
- [42] G. Moad, E. Rizzardo, S. H. Thang, *Polymer* **2008**, *49*, 1079–1131.
- [43] W. A. Braunecker, K. Matyjaszewski, *Prog. Polym. Sci.* **2007**, *32*, 93–146.
- [44] C. W. Bielawski, R. H. Grubbs, *Prog. Polym. Sci.* **2007**, *32*, 1–29.
- [45] J. Zhang, K. Liu, K. Mullen, M. Yin, *Chem. Commun.* **2015**, *51*, 11541–11555.
- [46] K. M.-C. Wong, N. Zhu, V. W.-W. Yam, *Chem. Commun.* **2006**, 3441–3443.
- [47] R. Büchner, C. T. Cunningham, J. S. Field, R. J. Haines, D. R. McMillin, G. C. Summerton, *J. Chem. Soc. Dalton Trans.* **1999**, 711–718.
- [48] W. B. Connick, R. E. Marsh, W. P. Schaefer, H. B. Gray, *Inorg. Chem.* **1997**, *36*, 913–922.
- [49] M. G. Hill, J. A. Bailey, V. M. Miskowski, H. B. Gray, *Inorg. Chem.* **1996**, *35*, 4585–4590.
- [50] J. A. Bailey, M. G. Hill, R. E. Marsh, V. M. Miskowski, W. P. Schaefer, H. B. Gray, *Inorg. Chem.* **1995**, *34*, 4591–4599.
- [51] R. H. Herber, M. Croft, M. J. Coyer, B. Bilash, A. Sahiner, *Inorg. Chem.* **1994**, *33*, 2422–2426.
- [52] T. K. Aldridge, E. M. Stacy, D. R. McMillin, *Inorg. Chem.* **1994**, *33*, 722–727.
- [53] H.-K. Yip, L.-K. Cheng, K.-K. Cheung, C.-M. Che, *J. Chem. Soc. Dalton Trans.* **1993**, 2933–2938.
- [54] V. M. Miskowski, V. H. Houlding, C. M. Che, Y. Wang, *Inorg. Chem.* **1993**, *32*, 2518–2524.
- [55] V. M. Miskowski, V. H. Houlding, *Inorg. Chem.* **1991**, *30*, 4446–4452.
- [56] H. Kunkely, A. Vogler, *J. Am. Chem. Soc.* **1990**, *112*, 5625–5627.
- [57] V. M. Miskowski, V. H. Houlding, *Inorg. Chem.* **1989**, *28*, 1529–1533.
- [58] C.-M. Che, K.-T. Wan, L.-Y. He, C.-K. Poon, V. W.-W. Yam, *J. Chem. Soc. Chem. Commun.* **1989**, 943–944.
- [59] C.-M. Che, L.-Y. He, C.-K. Poon, T. C.-W. Mak, *Inorg. Chem.* **1989**, *28*, 3081–3083.
- [60] J. W. Schindler, R. C. Fukuda, A. W. Adamson, *J. Am. Chem. Soc.* **1982**, *104*, 3596–3600.
- [61] S. Y.-L. Leung, W. H. Lam, V. W.-W. Yam, *Proc. Natl. Acad. Sci. USA* **2013**, *110*, 7986–7991.
- [62] H.-S. Lo, S.-K. Yip, N. Zhu, V. W.-W. Yam, *Dalton Trans.* **2007**, 4386–4389.
- [63] X. Yan, G. Liu, J. Hu, C. G. Willson, *Macromolecules* **2006**, *39*, 1906–1912.
- [64] J. Stadermann, H. Komber, M. Erber, F. Däbritz, H. Ritter, B. Voit, *Macromolecules* **2011**, *44*, 3250–3259.
- [65] T. Wei, J. H. Jung, T. F. Scott, *J. Am. Chem. Soc.* **2015**, *137*, 16196–16202.
- [66] M. Chen, H. Zhu, S. Zhou, W. Xu, S. Dong, H. Li, J. Hao, *Langmuir* **2016**, *32*, 2338–2347.
- [67] L. Zhang, R. Elupula, S. M. Grayson, J. M. Torkelson, *Macromolecules* **2016**, *49*, 257–268.
- [68] R. Joseph, A. Nkrumah, R. J. Clark, E. Masson, *J. Am. Chem. Soc.* **2014**, *136*, 6602–6607.
- [69] W. Lu, Y.-C. Law, J. Han, S. S.-Y. Chui, D.-L. Ma, N. Zhu, C.-M. Che, *Chem. Asian J.* **2008**, *3*, 59–69.

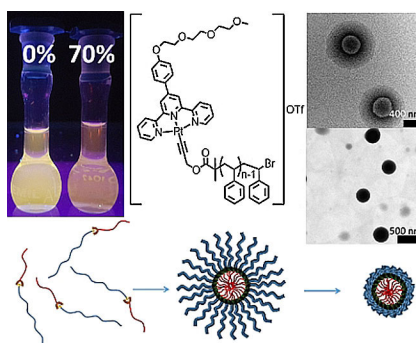
Manuscript received: January 26, 2017

Revised: February 28, 2017

Final Article published: ■ ■ ■, 0000

## FULL PAPER

**Go platinum:** A series of platinum(II)-containing polystyrene complexes has been synthesized and demonstrated to undergo self-assembly into different superstructures in various solvent mixtures with the stabilization of Pt...Pt and/or  $\pi$ - $\pi$  interactions, resulting in remarkable luminescence changes.



### Self-assembly

Heung-Kiu Cheng, Clive Yik-Sham Chung,  
Kaka Zhang, Vivian Wing-Wah Yam\*



Simple and Versatile Preparation of  
Luminescent Amphiphilic Platinum(II)-  
containing Polystyrene Complexes  
With Transformable Nanostructures  
Assisted by Pt...Pt and  $\pi$ - $\pi$   
Interactions

